Supplementary Material: Al-rich $Fe_{0.85}Al_{0.15}$(100), (110) and (111) surface structures

Zongbei Dai[1], Natalia Alyabyeva[1], Patrizia Borghetti[1], Stéphane Chenot[1], Pascal David[1], Alexey Koltsov[b], Gilles Renaud[c], Jacques Jupille[1], Gregory Cabailh[1], Rémi Lazzari[1,*]

[a] *CNRS, Sorbonne Université, Institut des NanoSciences de Paris, UMR 7588, 4 Place Jussieu, F-75005 Paris, France*
[b] *ArcelorMittal Maizières Research, voie Romaine, F-57280, Maizières-lès-Metz, France*
[c] *Université Grenoble Alpes, CEA, IRIG, MEM, F-38000 Grenoble, France*

[*] Corresponding author
Email address: remi.lazzari@insp.jussieu.fr (Rémi Lazzari)

Preprint submitted to Applied Surface Science *January 12, 2020*

1. Bulk truncation ball models of the body-centered cubic structure

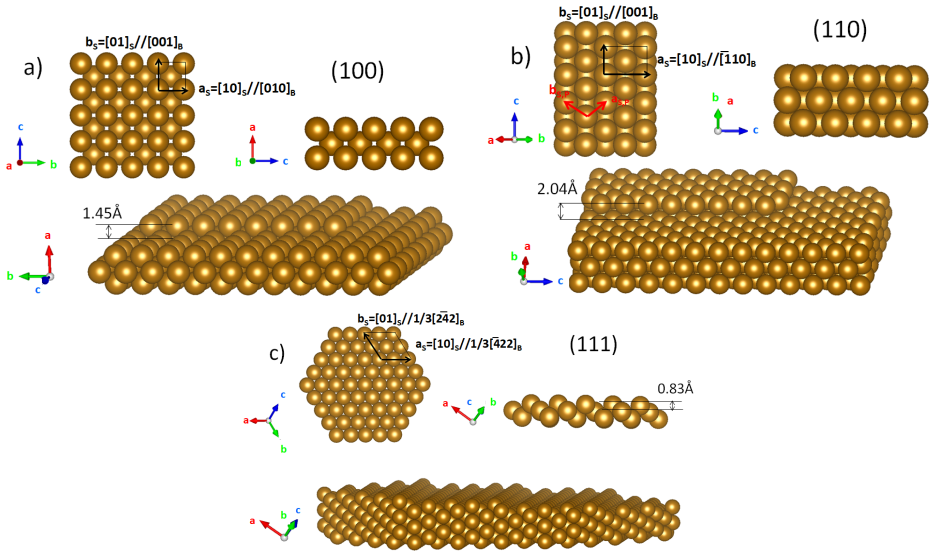

Figure S1: Atomic models of the a) (100), b) (110) and c) (111) bulk truncation of the body-centered cubic A_2 $Fe_{0.85}Al_{0.15}$ random alloy (lattice parameter $a_B = 2.89$ Å). Only the average atom is represented. The bulk cubic unit cell vectors $(\mathbf{a}_B, \mathbf{b}_B, \mathbf{c}_B)$ are displayed with colored arrows while black arrows correspond to the surface unit cell $(\mathbf{a}_S, \mathbf{b}_S)$ defined as (i) (100): $\mathbf{a}_S = \mathbf{b}_B$, $\mathbf{b}_S = \mathbf{c}_B$, $\mathbf{c}_S = \mathbf{a}_B$, (ii) (110): $\mathbf{a}_S = -\mathbf{a}_B + \mathbf{b}_B$, $\mathbf{b}_S = \mathbf{c}_B$, $\mathbf{c}_S = \mathbf{a}_B + \mathbf{b}_B$ ($a_S = \sqrt{2}a_B = 4.09$ Å, $b_S = a_B = 2.89$ Å), (iii) (111): $\mathbf{a}_S = (-4\mathbf{a}_B + 2\mathbf{b}_B + 2\mathbf{c}_B)/3$, $\mathbf{b}_S = (2\mathbf{a}_B - 4\mathbf{b}_B + 2\mathbf{c}_B)/3$, $\mathbf{c}_S = (\mathbf{a}_B + \mathbf{b}_B + \mathbf{c}_B)/2$ ($a_S = b_S = 2\sqrt{2}a_B/\sqrt{3} = 4.72$ Å). For the (110) surface, the primitive unit cell defined by $\mathbf{a}_{S,P} = (\mathbf{a}_S + \mathbf{b}_S)/2$ and $\mathbf{a}_{S,P} = (-\mathbf{a}_S + \mathbf{b}_S)/2$ from the rectangular centered one is indicated by red arrows. Top views along a) $[100]_B$, b) $[110]_B$, c) $[111]_B$; side views along a) $[010]_B$, b) $[\bar{1}10]_B$, c) $[01\bar{1}]_B$; the figures in perspective highlight the monolayer step. The atomic density per unit of surface is given by: $n_S = 1/a_B^2$, $n_S = \sqrt{2}/a_B^2$, $n_S = 3\sqrt{3}/4a_B^2$ for $(100), (110), (111)$ faces leading to $n_S(100) < n_S(111) < n_S(110)$.

2. $Fe_{0.85}Al_{0.15}(110)$ surface

The long-range ordered superstructure of $Fe_{0.85}Al_{0.15}(110)$ is present from one terrace to the other (Fig. S2) and does not appear as different domains, in agreement with the supercell observed by LEED and GIXD.

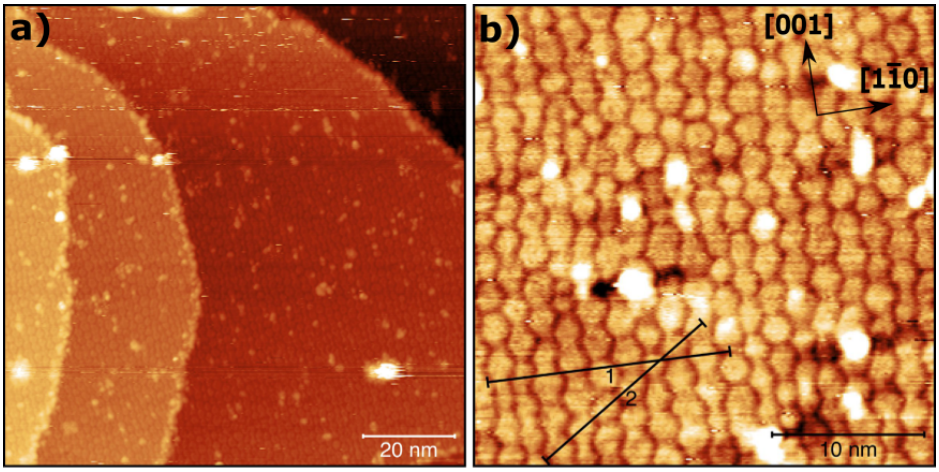

Figure S2: a) Large scale (100×100 nm^2, $U_b = 2.1$ V, $I_t = 0.2$ nA) and b) high resolution (30×30 nm^2, $U_b = 2.3$ V, $I_t = 0.2$ nA) STM images of the $Fe_{0.85}Al_{0.15}(110)$ surface annealed at 1150 K. Bright protrusions are due to contaminations from residual vacuum.

The $Fe_{0.85}Al_{0.15}(110)$ hexagonal-like surface reconstruction present at 2.5 V bias disappears at -2.5 V when the current tunnels from the the tip to the metal (Fig. S3-a). However, the apparent "network" structure present at -2.5 V on the bare surface (see Fig. S4) when the current tunnels through the tip-oxide-metal heterostructure is also observed when an oxide layer is formed on purpose. As highlighted by the change of contrast during scanning (Fig. S3-b), we believe that this "network" structure seen on the bare surface at negative bias is an artefact, due to the presence of an adsorbate on the tip and to the chemical composition of the surface (Fig. S4). The link to the local chemical composition of the reconstruction remains however unclear.

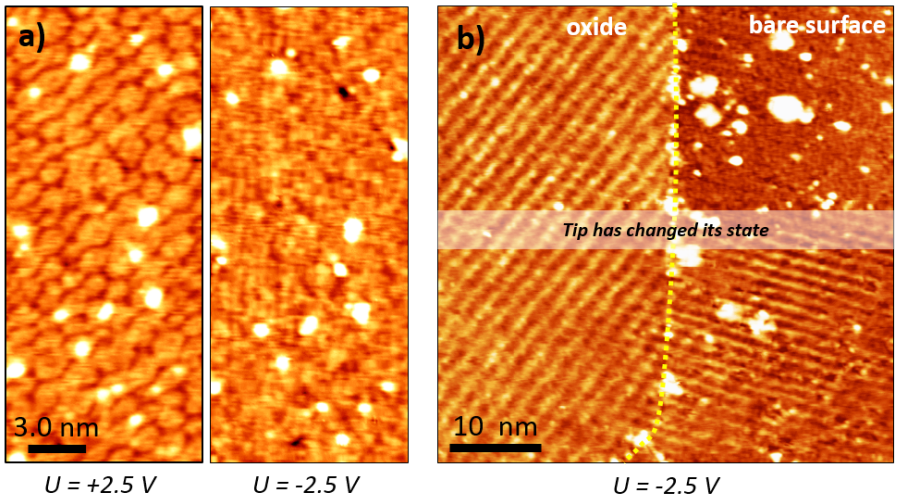

Figure S3: $Fe_{0.85}Al_{0.15}(110)$ STM images: a) surface reconstruction of the metallic surface at $U_b = 2.5$ V and -2.5 V ($I_t = 0.02$ nA) and b) two different tunneling regimes without (above) and with (below) adsorbate on the tip at the boundary between oxidized and bare surface.

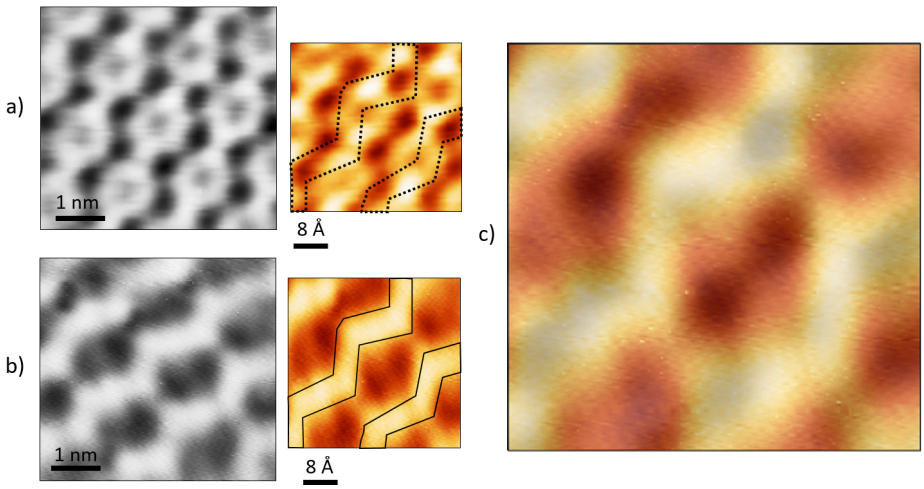

Figure S4: STM images (5×5 nm^2) of $Fe_{0.85}Al_{0.15}(110)$ surface reconstruction at $U_b = 2.5$ V and $I_t = 0.02$ nA: tip without a) and with b) adsorbate. The dotted lines in the close-up image of a) indicates how artefacts overlap with the surface reconstruction, indicated by solid line in the close-up of b). Superimposed images of both close-up images are in c).

3. $Fe_{0.85}Al_{0.15}(100)$ surface

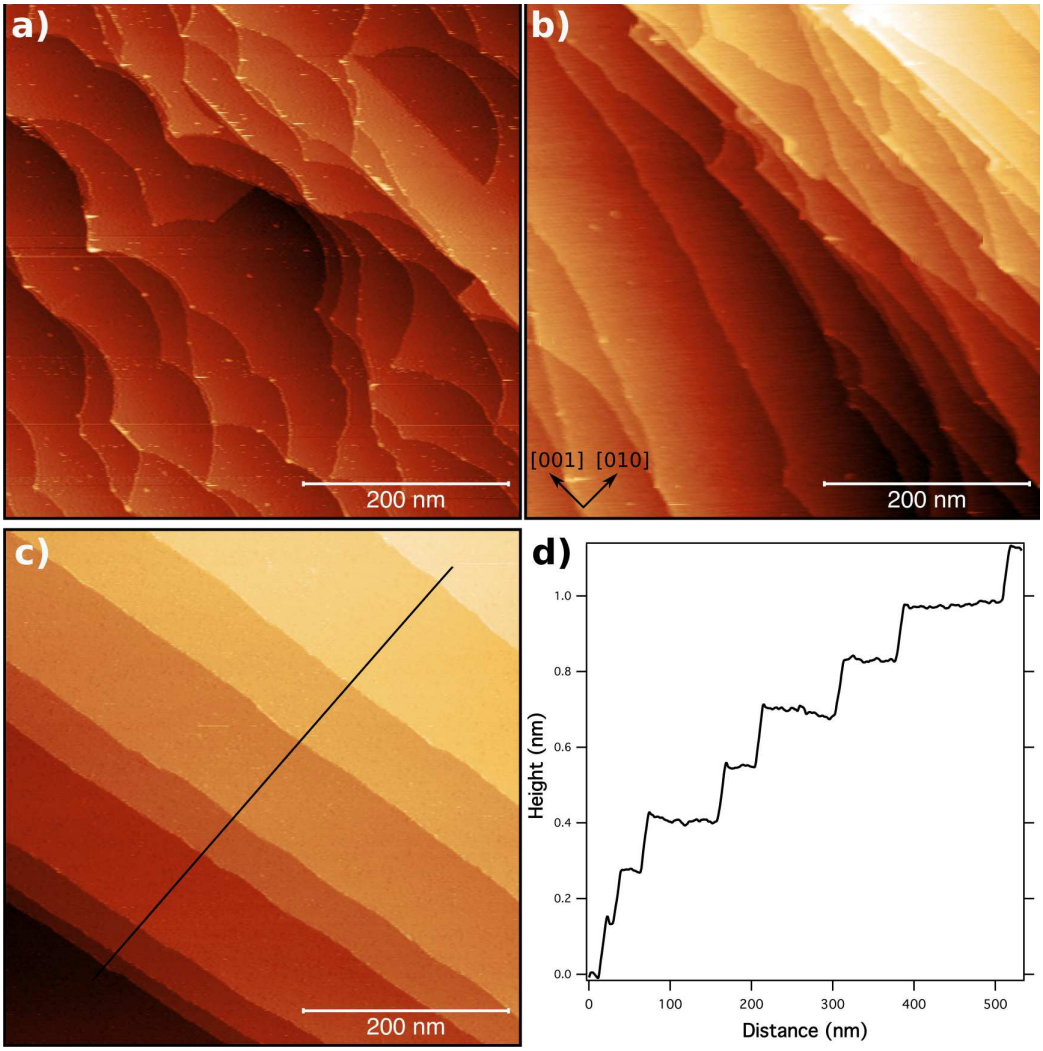

Figure S5: Large scale STM images (500×500 nm^2) of the $Fe_{0.85}Al_{0.15}(100)$ surface after annealing at three different temperatures: a) 1051 K ($U_b = 1.5$ V, $I_t = 0.4$ nA), b) 1078 K ($U_b = 0.8$ V, $I_t = 0.1$ nA), c) 1178 K ($U_b = -0.9$ V, $I_t = 0.3$ nA). d) Line profile drawn on the image c.

4. $Fe_{0.85}Al_{0.15}(111)$ surface

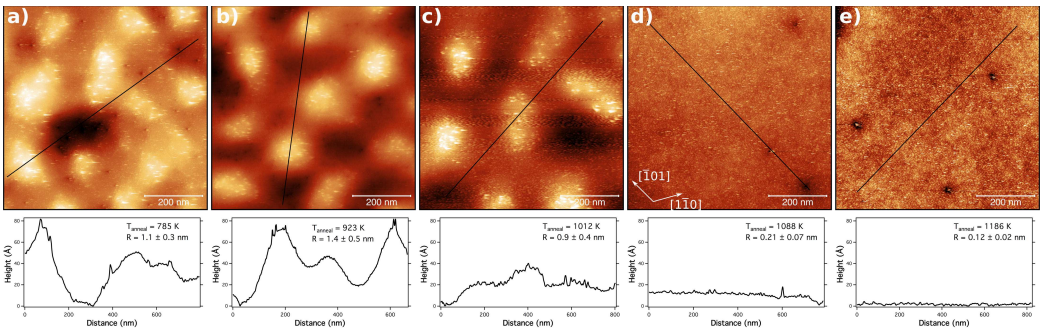

Figure S6: STM images (700×700 nm^2) of the $Fe_{0.85}Al_{0.15}(111)$ surface for different annealing temperatures as indicated on the figure. A typical line profile is drawn under each image and the roughness parameter R_a is also indicated. a) $U_b = -1.6$ V, $I_t = 0.4$ nA, b) $U_b = 1.5$ V, $I_t = 0.4$ nA, c) $U_b = -1.5$ V, $I_t = 0.4$ nA, d) $U_b = 1.6$ V, $I_t = 0.4$ nA, e) $U_b = 1.6$ V, $I_t = 0.4$ nA.

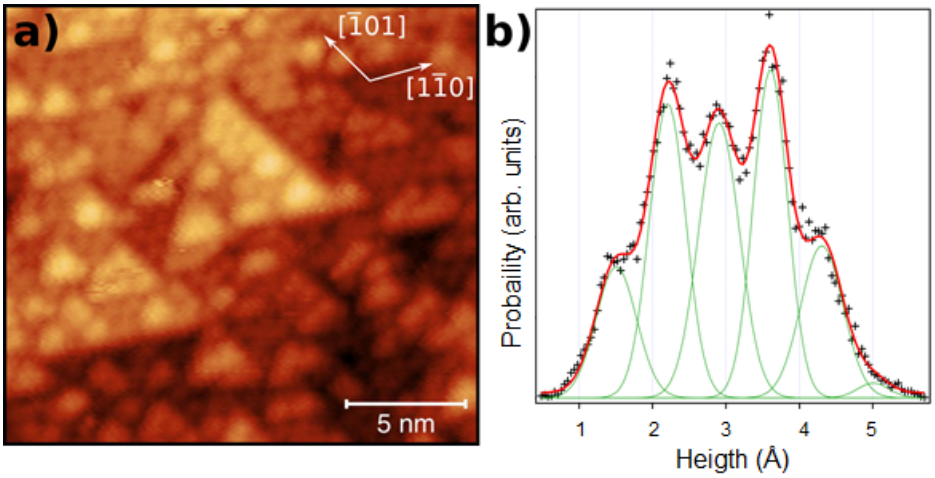

Figure S7: a) STM image (20×18 nm^2, $U_b = -1.6$ V, $I_t = 0.5$ nA) of the $Fe_{0.85}Al_{0.15}(111)$ surface annealed at 1173 K. b) Corresponding height histogram with its fit using several equidistant peaks. The number of peaks corresponds to two unit cells along the $[111]_B$ direction. Their spacing is close to the distance between atomic planes *i.e.* $a_B/2\sqrt{3} = 0.83$ Å.

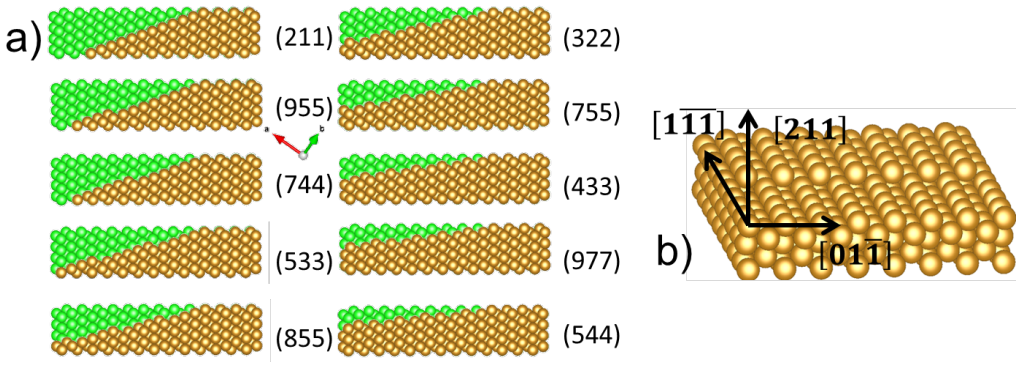

Figure S8: a) Ball models (brown spheres) of bcc vicinal surfaces normal to the $[01\bar{1}]$ direction. Green balls stand for missing atoms of the full (111) surface. At the opposite of face-centered cubic (fcc) (111) vicinal surfaces which are staircases of single stepped compact (111) planes of decreasing widths with the miscut, the bcc (111) vicinal ones are more complex. They are made out of (211) local facets separated by single steps of heigth $a_B/\sqrt{3}$ and aligned along the $[01\bar{1}]_B$ directions. b) View in perspective of the (211) bcc surface showing a step edge and the protuding atom rows along the $[1\bar{1}\bar{1}]_B$ direction leading to open step edges with two-fold coordinated atom.

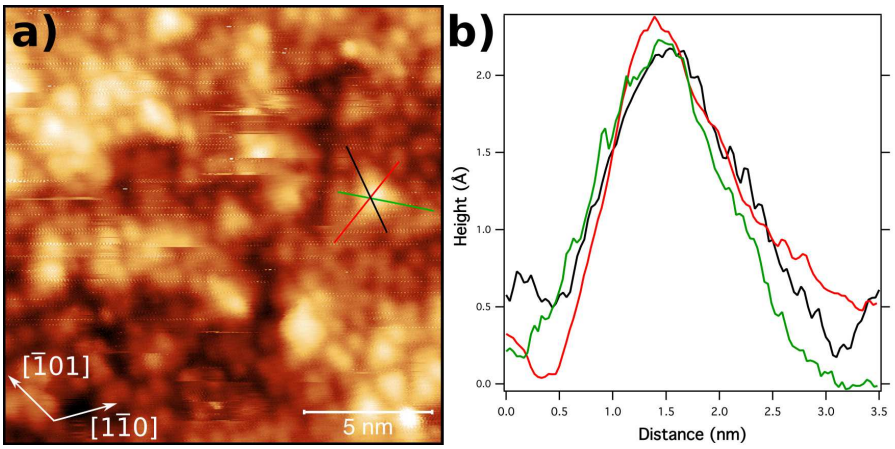

Figure S9: STM images of the $Fe_{0.85}Al_{0.15}(111)$ surface (17×17 nm^2, $U_b = -1.2$ V, $I_t = 0.4$ nA) annealed at 785 K. The line profiles are represented on the right with the same color code.

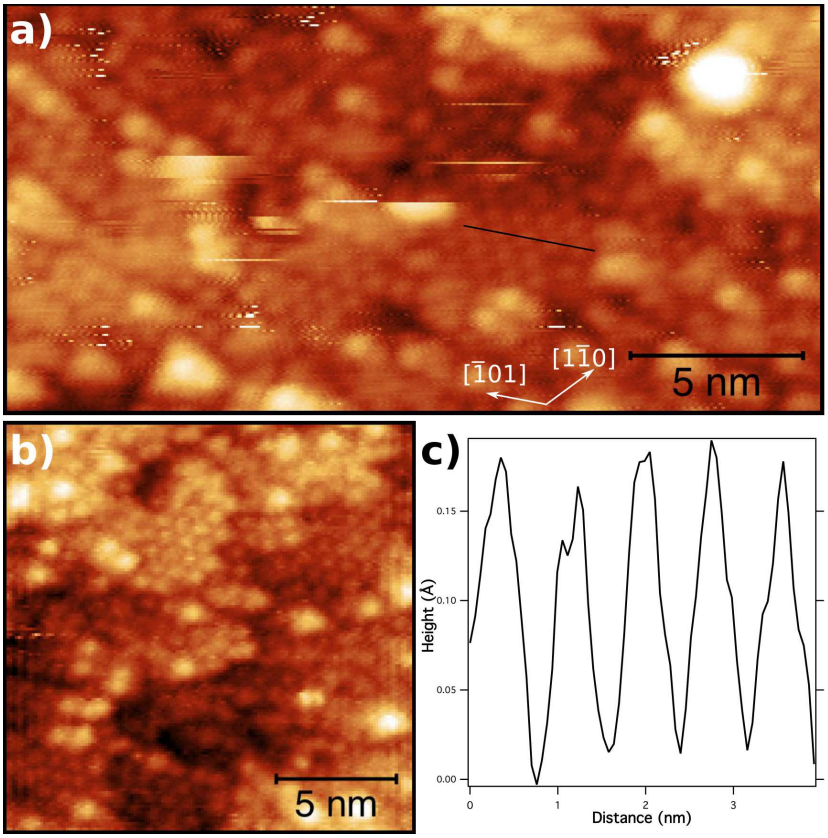

Figure S10: High resolution STM images of the $Fe_{0.85}Al_{0.15}(111)$ surface annealed at 785 K. a) 23.5×11.5 nm^2, $U_b = -1.6$ V, $I_t = 0.4$ nA, b) 17×17 nm^2, $U_b = -1.6$ V, $I_t = 0.5$ nA, c) Line profile corresponding to the black line of figure-a.